JVI Journals.ASM.org

Nectin-4-Dependent Measles Virus Spread to the Cynomolgus Monkey Tracheal Epithelium: Role of Infected Immune Cells Infiltrating the Lamina Propria

Marie Frenzke,[a] Bevan Sawatsky,[b]* Xiao X. Wong,[b] Sébastien Delpeut,[b] Mathieu Mateo,[a] Roberto Cattaneo,[a] Veronika von Messling[b,c]

Department of Molecular Medicine, Virology and Gene Therapy Graduate Track, Mayo Clinic College of Medicine, Rochester, Minnesota, USA[a]; INRS-Institut Armand-Frappier, University of Quebec, Laval, Quebec, Canada[b]; Emerging Infectious Diseases Program, Duke-NUS Graduate Medical School, Singapore, Singapore[c]

After the contagion measles virus (MV) crosses the respiratory epithelium within myeloid cells that express the primary receptor signaling lymphocytic activation molecule (SLAM), it replicates briskly in SLAM-expressing cells in lymphatic organs. Later, the infection spreads to epithelia expressing nectin-4, an adherens junction protein expressed preferentially in the trachea, but how it gets there is not understood. To characterize the mechanisms of spread, we infected groups of 5 or 6 cynomolgus monkeys (*Macaca fascicularis*) with either a wild-type MV or its "N4-blind" derivative, which is unable to enter nectin-4-expressing cells because of the targeted mutation of two hemagglutinin residues. As expected, both viruses caused similar levels of immunosuppression, as monitored by reductions in white blood cell counts and lymphocyte proliferation activity. However, monkeys infected with the N4-blind MV cleared infection more rapidly. Wild-type virus-infected monkeys secreted virus, while marginal virus titers were detected in tracheal lavage fluid cells of N4-blind MV-infected hosts. Analyses of tracheal rings obtained at necropsy (day 12) documented widespread infection of individual cells or small cell clusters in the subepithelial lamina propria of monkeys infected with either virus. However, only wild-type MV spread to the epithelium, forming numerous infectious centers comprised of many contiguous columnar cells. Infected CD11c$^+$ myeloid (macrophage or dendritic) cells were frequently observed in the lamina propria below epithelial infectious centers. Thus, MV may use myeloid cells as vehicles not only immediately after contagion but also to infect epithelia of tissues expressing nectin-4, including the trachea.

Measles virus (MV) infections remain a major cause of vaccine-preventable childhood deaths worldwide (1, 2). However, vaccine fatigue in industrialized countries and health care delivery limitations in the developing world are major challenges for eradication (3). The highly contagious nature of MV makes it difficult to interrupt transmission during an outbreak (4, 5). In the absence of antiviral drugs, vaccination campaigns, isolation of patients and contacts, and supportive therapy are the only available public health measures to stop MV reemergence.

In addition to humans, several nonhuman primate species, including rhesus and cynomolgus monkeys, are naturally susceptible to MV infection and develop symptoms that reproduce those seen in humans (6, 7). Experimental inoculation of rhesus and cynomolgus monkeys with recombinant MV, either expressing reporter proteins or carrying specific defects, has greatly enhanced our understanding of MV pathogenesis (8, 9). After inoculation of the host with aerosolized virus, infection is detected first in resident immune cells of the lower respiratory tract (10). The virus then spreads to lymph nodes, where it infects a broad range of immune cells expressing the signaling lymphocytic activation molecule (CD150/SLAM) (8, 11, 12). Infected circulating immune cells disseminate the infection throughout the lymphatic system, followed by spread to epithelial tissues (13, 14). Two groups recently identified the long-sought epithelial receptor (EpR) as nectin-4 (N4) (15, 16). Nectin-4 is expressed preferentially in the tracheobronchial epithelium (17, 18), the ideal location for aerosol droplet release through coughing and sneezing (15, 19), accounting for the observation that MV is the human virus with the highest reproductive rate (20).

Even before identification of nectin-4 as the EpR, a recombinant wild-type MV carrying a hemagglutinin with mutations that abolish EpR-mediated entry was generated and inoculated into rhesus monkeys (21). Hosts infected with the selectively EpR-blind MV developed clinical symptoms similar to those developed by wild-type MV-infected hosts, but they did not shed virus (21). However, since the tracheal localization of EpR/nectin-4 was not known, questions regarding the spread of infection in the tracheal epithelium were not addressed. Moreover, comparison of virus-shedding efficiencies was based on a historic control group rather than a simultaneously infected group (10, 21).

To directly compare infections of the wild type and its EpR/nectin-4-blind derivative and to characterize viral spread to the tracheal epithelium, we inoculated groups of 5 or 6 cynomolgus monkeys. After comparison of the kinetics and extents of infection in circulating immune cells and lymph nodes as well as in upper airway secretions, monkeys were sacrificed at the peak of clinical disease (6), and epithelial and immune tissues were harvested. Their analysis revealed how infected myeloid cells infiltrating the lamina propria of the trachea may spread the infection to the apical epithelium.

Received 31 October 2012 **Accepted** 7 December 2012
Published ahead of print 19 December 2012
Address correspondence to Roberto Cattaneo, Cattaneo.Roberto@mayo.edu.
* Present address: Bevan Sawatsky, University of Texas Medical Branch, Department of Microbiology and Immunology, Galveston, Texas, USA.
Copyright © 2013, American Society for Microbiology. All Rights Reserved.
doi:10.1128/JVI.03037-12

MATERIALS AND METHODS

Cells and viruses. Vero cells stably expressing human SLAM (Vero/hSLAM cells) (22), kindly provided by Y. Yanagi (Kyushu University, Fukuoka, Japan), were maintained in Dulbecco's modified Eagle medium (DMEM; Invitrogen, Burlington, Ontario, Canada) supplemented with 5% heat-inactivated fetal bovine serum (FBS; Life Science, Grand Island, NY) and 0.5 mg/ml of G418 (Invitrogen). The enhanced green fluorescent protein (EGFP)-expressing wild-type MV strain IC323 (23, 24) (referred to here as parental MV) and its N4-blind derivative, MV-N4^{blind} (15, 21), were propagated in Vero/hSLAM cells, and titers were determined by a limiting dilution method and expressed as 50% tissue culture infective doses ($TCID_{50}$). We note that a previous rhesus monkey infection study was based on variants of these viruses that did not express EGFP (21).

Animal experiments. Female cynomolgus monkeys (*Macaca fascicularis*) without preexisting immunity against MV were obtained from the Health Canada colony in Ottawa. The animals were housed in accordance with guidelines of the Canadian Council for Animal Care and the American Association for Accreditation of Laboratory Animal Care. All experiments were approved by the Institutional Animal Care and Use Committee of the INRS-Institut Armand-Frappier. Groups of five or six animals were infected intranasally with $10^{4.5}$ $TCID_{50}$ of MV-N4^{blind} or the parental MV strain, respectively. The animals were monitored daily for clinical signs, including anorexia, depression, diarrhea, and skin rash. On days 3, 6, 9, and 12, animals were anesthetized with ketamine (Pfizer, Kirkland, Quebec, Canada) and weighed, and blood samples were collected. On days 6, 9, and 12, the animals were then intubated and maintained with isoflurane (Baxter Corporation, Mississauga, Ontario, Canada) to obtain lymph node biopsy specimens, and tracheal lavage fluid was collected before removal of the tracheal tube. All animals were sacrificed on day 12 after infection, and tissues were harvested for histological analyses and RNA isolation.

Virus quantification. To determine virus titers in peripheral blood mononuclear cells (PBMCs), white blood cells (WBC) were isolated from EDTA-treated blood samples by use of ACK lysis buffer (Invitrogen). The cells were counted and then cocultivated with Vero/hSLAM cells in serial 10-fold dilutions. Virus titers were read after 5 days of incubation and expressed as $TCID_{50}/10^6$ cells. For quantification of virus in lymph node biopsy specimens, samples were weighed and a maximum of 0.5 g was homogenized in 500 μl of DMEM with 10× penicillin-streptomycin (Invitrogen) for two rounds of 10 s each at 6 m/s, using a FastPrep-24 tissue homogenizer (MP-Biomedicals, Santa Ana, CA), followed by a quick spin. Virus titers in lysate supernatant and tracheal lavage fluid samples were determined by limiting dilution and expressed as $TCID_{50}$ per g tissue and ml fluid, respectively.

Immune response assessment. The total white blood cell count was quantified from analysis of EDTA-treated blood samples after a 1:100 dilution in 3% acetic acid. To evaluate the ability of PBMCs to proliferate upon nonspecific stimulation, Ficoll-purified PBMCs were activated with 1 μg/ml phytohemagglutinin (PHA), and the extent of bromodeoxyuridine (BrdU) incorporation was quantified using a cell proliferation enzyme-linked immunosorbent assay (ELISA) kit for BrdU (Roche, Mississauga, Ontario, Canada).

Immunostaining. Tissue samples were collected and fixed in 4% paraformaldehyde (Sigma, St. Louis, MO) for at least 48 h. Fixed samples were embedded in paraffin and cut into 5-μm-thick sections. Slides were stained using monoclonal antibodies against measles virus nucleoprotein (Millipore, Burlington, MA), CD11c (Leica Biosystems, Buffalo Grove, IL), and CD45 (Dako, Carpinteria, CA) in combination with reagents of a NovoLink Min polymer detection system (Leica Biosystems), which contained the 3,3′-diaminobenzidine (DAB) chromogen and a hematoxylin counterstain. Staining for CD11c and CD45 required antigen retrieval treatment (Dako) before staining. The slides were mounted in Vectamount (Vector Laboratories, Burlingame, CA).

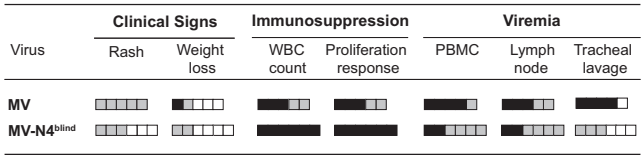

FIG 1 Clinical signs, immunosuppression parameters, and viral loads associated with wild-type and N4-blind MV infections. Groups of 5 or 6 female macaques were inoculated intranasally with $10^{4.5}$ $TCID_{50}$ of wild-type or N4-blind MV. Clinical signs were assessed daily, and tracheal lavage fluid and blood samples were collected every third day. Each box represents one animal; the strongest effects observed during the study are indicated. Grading (general) is indicated as follows: white filling, no change from noninfected controls; gray, intermediate change; black, strong change. Grading of each parameter is as follows: rash, none, mild/localized, or severe/generalized; weight loss, none, 1 to 5%, or >5%; WBC count (decrease from 100% baseline measured for the individual host), <33%, 33 to 66%, or >66%; *in vitro* proliferation activity (ratio of mitogen-stimulated and nonstimulated cells; decrease from highest value measured for the individual host), <33%, 33 to 66%, or >66%; number of infected cells in 10^6 PBMCs, none, 1 to 100 $TCID_{50}$, or >100 $TCID_{50}$; virus titer in lymph node biopsy specimens, none, 1 to 100 $TCID_{50}$, or >100 $TCID_{50}$ per mg tissue; and infected virus titer in tracheal lavage fluid, none, 1 to 100 $TCID_{50}$, or >100 $TCID_{50}$ per sample.

Statistical analyses. Prism (Graph Pad, La Jolla, CA) was used to identify statistically significant differences between the groups by unpaired Student's *t* test.

RESULTS

N4-blind MV is as virulent and immunosuppressive as the wild type in cynomolgus monkeys. A previous study compared clinical signs, immunosuppression parameters, and viremia levels of rhesus monkeys infected with a variant of the N4-blind MV that did not express EGFP (21) with those observed for a historic control group infected with the isogenic wild-type virus; however, virus release in the airways had to be compared with that observed in another study, which used MV-IC323-EGFP (8). To directly compare virulence, immunosuppression, and epithelial infection in hosts inoculated with viruses differing in only two residues of the attachment protein, we infected groups of 5 or 6 cynomolgus monkeys in parallel. The body weights of the hosts were recorded daily; blood samples were collected on day 3, to capture the early phase of systemic dissemination, and on days 6, 9, and 12, to follow progression of viremia and to quantify immunosuppression. In addition, lymph node biopsy specimens and tracheal lavage fluid were obtained at 6, 9, and 12 days.

While all hosts in the wild-type MV-infected group developed a mild rash on days 9 to 12, only three of the six N4-blind MV-infected hosts presented with rash (Fig. 1, left column). In light of the previously reported contribution of aggregates of infected inflammatory cells in close proximity to hair follicles to the observed rash (8), this difference likely reflects a more rapid clearance of the virus from immune cells rather than a lack of infection of keratinocytes. Most monkeys experienced little to no change in body weight (Fig. 1, second column). No sign of depression or respiratory or gastrointestinal involvement was documented (data not shown).

Virus was first isolated from PBMCs on day 6. At this time point, while three of five MV-infected hosts were positive, only one of the six hosts in the N4-blind MV-infected group was positive (Fig. 2A). Cell-associated viremia was detected in all hosts on day 9, at very similar average levels for both groups (Fig. 2A).

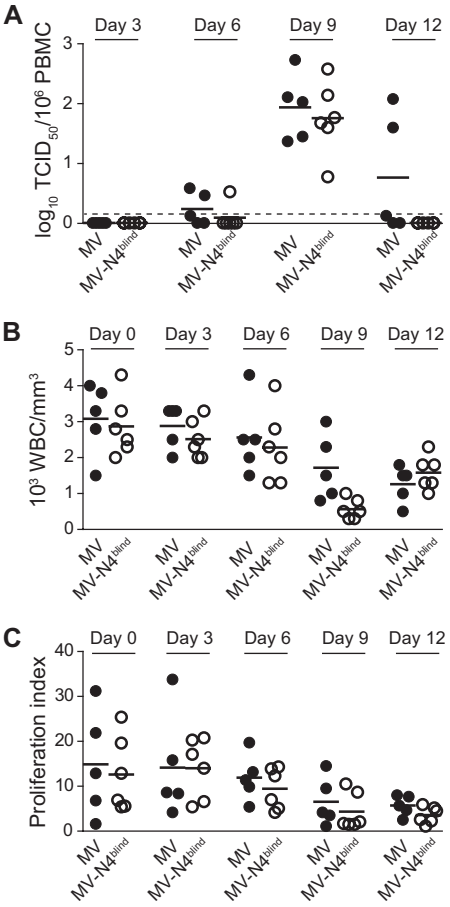

FIG 2 Quantitative analyses of cell-associated viremia and immunosuppression levels in hosts infected with wild-type or N4-blind MV. Cell-associated viremia (A), WBC counts (B), and *in vitro* lymphocyte proliferation activity levels (C) were documented before inoculation and at days 3, 6, 9, and 12 after inoculation. Cell-associated viremia is expressed as the $\log_{10}$ $TCID_{50}$ per 10^6 PBMCs, and the detection limit is indicated as a dashed line. The WBC count is expressed as the number (10^3) of cells per mm^3, and the proliferation index reflects the ratio of BrdU incorporation in PHA-stimulated and nonstimulated PBMCs. Horizontal thick black lines indicate the group means.

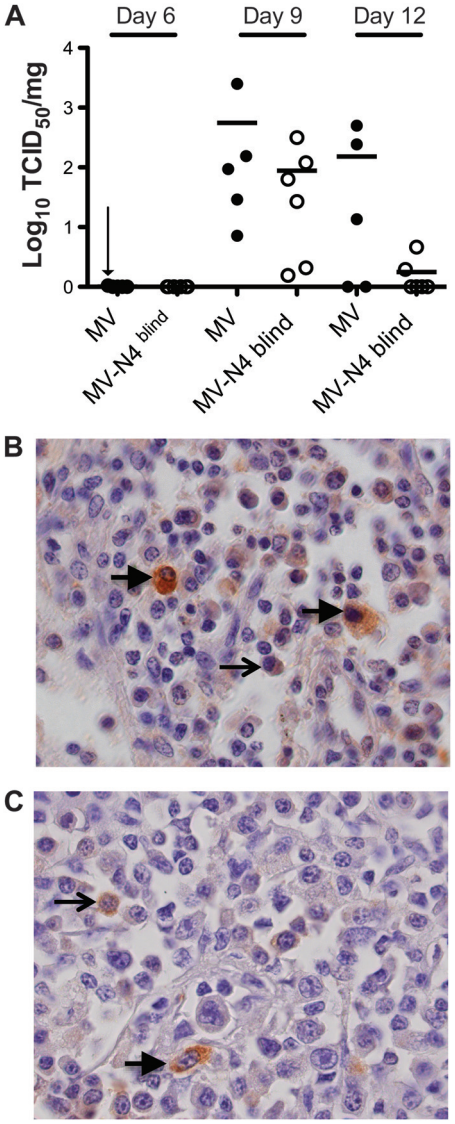

FIG 3 Virus titers and analysis of infected cell types in inguinal lymph nodes. Inguinal lymph nodes were surgically removed from animals on days 6 and 9 after inoculation or collected during necropsy on day 12. (A) Cell-associated virus titers over the course of the infection. Titers are expressed as $\log_{10}$ $TCID_{50}$/mg of tissue. Horizontal thick black lines indicate the group means. The detection limit was 1 $TCID_{50}$/mg of tissue. A vertical arrow indicates one value just above the detection limit. (B and C) Nucleocapsid-positive cells in lymph nodes collected during necropsy from animals infected with the wild-type (B) or N4-blind (C) MV. Paraffin sections were stained with an MV nucleoprotein-specific antibody, counterstained with hematoxylin, and photographed at a magnification of ×1,000. Arrows indicate lymphocytes (thin arrows) or macrophages (thick arrows).

However, while all hosts infected with the N4-blind virus had cleared it by day 12, three hosts infected with MV were still positive at that time point, with two monkeys maintaining the titers seen on day 9 (Fig. 2A).

WBC counts and lymphocyte proliferation responses were measured as immunosuppression parameters. Figure 2B documents a progressive drop in WBC count in hosts infected with either virus over time, with an average of about 50% WBC retained 12 days after inoculation. Concurrently, the lymphocyte proliferation index in response to PHA stimulation dropped 2- to 3-fold (Fig. 2C) in monkeys infected with either virus. Neutralizing antibodies were detected only on day 12, reaching average titers of around 1:20 in both groups (data not shown; low titers are expected at this early time point). Thus, the N4-blind virus was as immunosuppressive as MV. Taken together (Fig. 1), these results indicate similar overall virulence and immunosuppressive capacities of both viruses in cynomolgus monkeys, consistent with the results of a study of rhesus monkeys (21).

Lack of epithelial infection correlates with more rapid virus clearance. Previous studies based on wild-type MV-infected rhesus or cynomolgus macaques documented early and brisk infection of the immune organs (8). To compare the extents and kinetics of infection of the wild-type and N4-blind MV without sacrificing monkeys at early time points, we performed inguinal lymph node biopsies on days 6 and 9. We also collected inguinal lymph nodes at necropsy, on day 12. We quantified virus titers of all these materials and performed immunohistochemical staining of viral antigen in tissue sections.

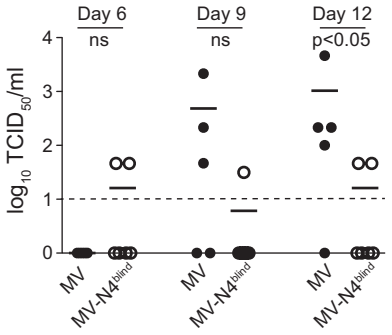

FIG 4 Virus shedding into the upper respiratory tract. Tracheal lavage fluid samples were collected from each animal on days 6, 9, and 12 postinfection. Virus titers were determined by limiting dilution and expressed as $\log_{10}$ $TCID_{50}$/ml. Horizontal thick black lines indicate the group means. The dashed line indicates the detection limit. ns, not significant.

Figure 3A documents that on day 6, cell-associated virus was detected in only one wild-type virus-infected monkey, just above the limit of detection of 1 $TCID_{50}$/mg of tissue. On day 9, wild-type infectivity was about 550 times above the detection level, on average, and the average infectivity of N4-blind MV was 6 times lower. On day 12, three hosts infected with the wild type still had titers of 10- to 100-fold over the detection level, while only two hosts infected with N4-blind MV still had detectable titers.

At necropsy, infected cells were detected throughout the lymph node, as shown by immunostaining with a viral nucleocapsid antibody for one host infected with the wild type (Fig. 3B) and one infected with N4-blind MV (Fig. 3C). Infected cells had myeloid (thick arrows) or lymphoid (thin arrows) morphology. Together with the virus replication levels documented for PBMCs, these results indicate that even though wild-type and N4-blind MV rep-

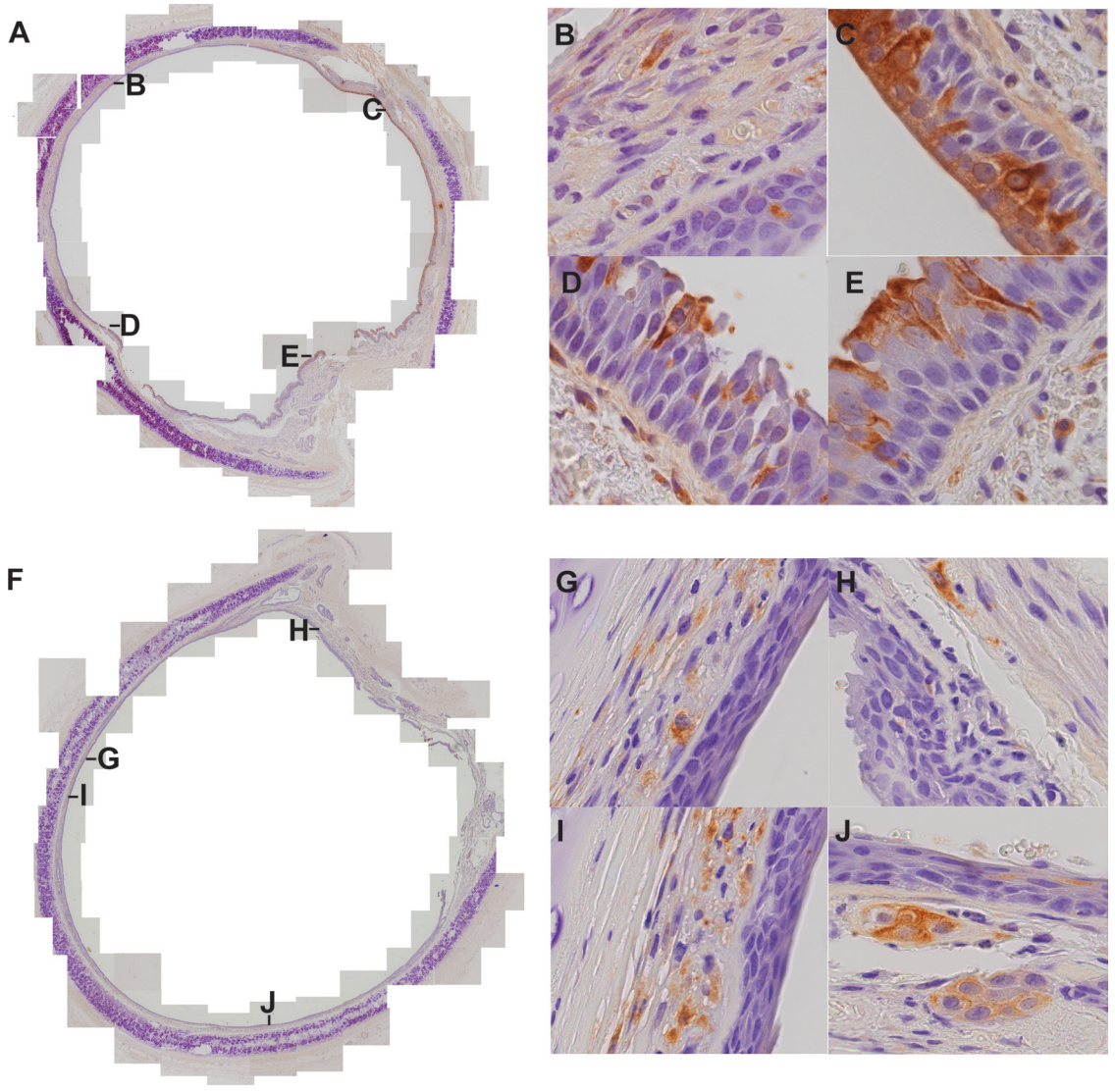

FIG 5 Localization of wild-type and N4-blind MV infections in tracheal rings. Paraffin-embedded tracheal sections from wild-type (A to E) or N4-blind (F to J) MV-infected animals were stained with a nucleocapsid-specific antibody revealed with the brown chromogen DAB and counterstained with hematoxylin. Composite pictures (A and F) were assembled from overlapping areas photographed at a magnification of ×200. Four examples of areas of infection (B to E and G to J) were photographed at a magnification of ×1,000. The locations of these areas are indicated with the respective letters in the composite views. Individual views covered 700 cells (counted nuclei), on average.

TABLE 1 Distribution of infection in the apical epithelium, lower pseudostratified epithelium (LPE), and lamina propria in hosts infected with MV or N4-blind MV

Virus	Animal no.	No. of viewed areas	Tissue	No. of areas with indicated no. of cells[a]			
				0	1–5	6–10	>10
MV	2	30	Epithelium	9	6	3	12
	2	30	LPE	13	11	3	3
	2	30	Lamina propria	22	5	3	0
	40	25	Epithelium	23	1	1	0
	40	25	LPE	25	0	0	0
	40	25	Lamina propria	20	4	1	0
	81	20	Epithelium	5	8	4	3
	81	20	LPE	13	5	2	0
	81	20	Lamina propria	12	6	2	0
	44	27	Epithelium	16	5	4	2
	44	27	LPE	16	9	2	0
	44	27	Lamina propria	20	6	1	0
	57	33	Epithelium	24	8	0	1
	57	33	LPE	30	3	0	0
	57	33	Lamina propria	27	6	0	0
Total		135	Epithelium	77	28	12	18
		135	LPE	97	28	7	3
		135	Lamina propria	101	27	7	0
MV-N4^{blind}	34	29	Epithelium	29	0	0	0
	34	29	LPE	26	3	0	0
	34	29	Lamina propria	25	3	1	0
	79	28	Epithelium	27	1	0	0
	79	28	LPE	27	1	0	0
	79	28	Lamina propria	18	8	2	0
	104	26	Epithelium	26	0	0	0
	104	26	LPE	20	6	0	0
	104	26	Lamina propria	19	6	1	0
	15	29	Epithelium	29	0	0	0
	15	29	LPE	25	4	0	0
	15	29	Lamina propria	16	10	3	0
	33	30	Epithelium	28	1	1	0
	33	30	LPE	25	5	0	0
	33	30	Lamina propria	27	3	0	0
	46	27	Epithelium	26	1	0	0
	46	27	LPE	26	1	0	0
	46	27	Lamina propria	20	7	0	0
Total		169	Epithelium	165	3	1	0
		169	LPE	149	20	0	0
		169	Lamina propria	125	37	7	0

[a] Slides were scored in a blind manner.

licate to similar levels in immune cells, a lack of epithelial cell infection correlates with more rapid clearance of N4-blind MV.

Efficient shedding into the upper respiratory tract requires epithelial infection. In the previous rhesus monkey study, no virus was detected in the airways of hosts infected with N4-blind MV (21). While another study reported wild-type MV isolation from the airways of rhesus and cynomolgus macaques on days 6 and 9 after inoculation (8), virus shedding efficiencies were not compared for simultaneously infected groups.

To allow direct comparisons, we performed tracheal lavage on all wild-type (Fig. 4, MV data) and N4-blind MV-infected animals 6, 9, and 12 days after inoculation. While none of the MV-infected monkeys had virus in their tracheal lavage fluid on day 6, titers 5 to 200 times over the detection level were documented for three of five hosts on day 9, coinciding with the onset of rash (Fig. 4, MV). At the peak of epithelial infection on day 12, titers 10 to 500 times over the detection level were detected in four hosts, resulting in a statistically significant difference ($P = 0.04$) between the wild-type and N4-blind MV-infected groups (Fig. 4, day 12).

Remarkably, for one N4-blind MV-infected host, low virus titers were documented throughout the study; for another N4-blind MV-infected host, low virus titers were detected on day 6, and for yet another host, they were detected on day 12 (Fig. 4, MV-N4^{blind}). While we do not have a definitive explanation for these observations, we note that low levels of secretion were detected already at day 6, before the epithelial phase of virus replication, and may thus reflect infected immune cells secreted from microabrasions caused by the tracheal tube used for the lavage

procedure. While in the rhesus monkey study the airway titers of wild-type virus were slightly higher (21), altogether these data indicate that epithelial infection is a prerequisite for efficient virus shedding into the upper respiratory tract.

In tracheal infections, only wild-type MV spreads efficiently to the epithelium. To compare replication of the wild-type and N4-blind viruses in the trachea, this organ was collected at necropsy from all hosts infected with either virus. Replication of both viruses was compared in the apical epithelial layer, the underlying pseudostratified epithelium, and the basal lamina (lamina propria). To this end, tracheal rings were stained with a nucleocapsid antibody and counterstained with hematoxylin. Localization of nucleocapsid-positive cells was documented qualitatively and quantitatively. Representative composite micrographs and close-up analyses of virus distributions are presented in Fig. 5.

Composite pictures of tracheal rings documented strikingly different localizations of wild-type (Fig. 5A) and N4-blind (Fig. 5F) MV infections. Only in wild-type MV-infected hosts were nucleocapsid-positive cells found in the apical epithelium, within infectious centers comprised of many contiguous columnar cells (close-up sections of Fig. 5C to E). In addition, in monkeys infected with MV, individual infected cells or small infected cell clusters were found in the lamina propria (Fig. 5B to E). In N4-blind MV-infected animals, the lamina propria pattern of infection recapitulated the infection pattern with MV (Fig. 5F to J), but infections of the apical epithelium were very rare.

To compare the frequencies of infections in the lamina propria and apical epithelium of MV- and N4-blind MV-infected monkeys, we quantified the number of infected cells from two different tracheal rings from each monkey. We counted infected cells within 25 to 30 views for each monkey, defining four infection levels: 0, 1 to 5, 6 to 10, and more than 10 infected cells per view and per type of tissue. Table 1 lists these data. Infection levels were measured in 135 views of tracheas from MV-infected hosts and 169 views of tracheas from N4-blind MV-infected hosts; the results are visualized in the charts of Fig. 6.

For MV-infected monkeys, at least one infected cell per view was identified in the lamina propria areas in 34 of 135 views (25%) (Fig. 6, top left chart). For N4-blind MV-infected animals, at least one infected cell was found in 44 of 169 views (26%) (Fig. 6, bottom left chart). Thus, levels of infection in the lamina propriae of animals inoculated with both viruses were equivalent.

On the other hand, while nucleocapsid-positive cells in epithelia of MV-infected animals were identified in 58 of 135 views (43%) (Fig. 6, top right chart), in epithelial views from N4-blind MV-infected animals, nucleocapsid staining was documented in 4 of 169 views (2%) (Fig. 6, bottom right chart). Thus, while similar levels of cells infected with wild-type MV or its N4-blind derivative were detected in the lamina propria of the trachea 12 days after inoculation, only wild-type MV replicated efficiently in the epithelium.

Myeloid cells may deliver MV to the tracheal epithelium. In the lamina propria, virus replication was confined to individual cells or small clusters of cells. Knowing that immune cells infiltrate the lamina propria, we stained consecutive slides with antibodies against the viral nucleocapsid, the monocyte/macrophage and dendritic cell marker CD11c, and the general leukocyte marker CD45. Figure 7A is a composite picture of a tracheal ring from a wild-type MV-infected host, stained with CD11c-specific antibodies. This analysis documents that $CD11c^+$ cells are well represented below the epithelial layer. Figure 7B documents a large, strongly nucleocapsid-stained area of the epithelium. In the nearby lamina propria, both $CD11c^+$ (Fig. 7C) and $CD45^+$ (Fig. 7D) cells were detected. While analyses of consecutive slides (5 μm thick) rarely allow one to make definitive statements about double staining of individual cells, it appears that certain $CD11c^+$ cells in the submucosa were also nucleocapsid positive (arrows in Fig. 7B and C). The apparently lower frequency of $CD45^+$ cells likely reflects a lower cross-reactivity of the human CD45-specific antibody with the cynomolgus macaque CD45 proteins, making it difficult to assess the extent of infection in non-macrophage/dendritic immune cells. Nonetheless, these analyses support a role of infiltrating immune cells, and in particular of $CD11c^+$ macrophages or dendritic cells, in transferring the infection from the lamina propria to the tracheal epithelium.

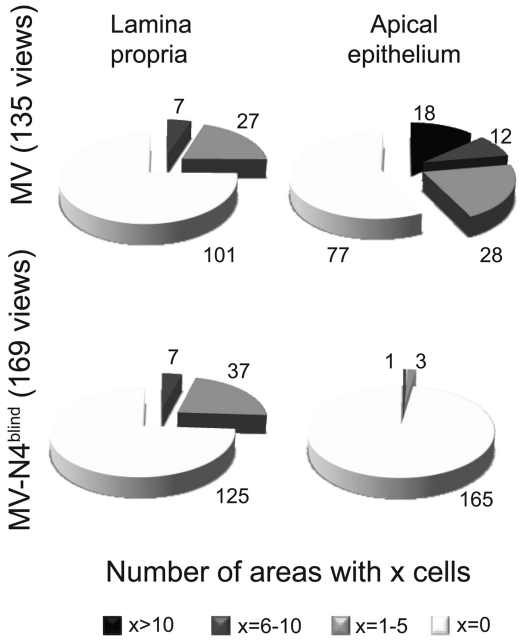

FIG 6 Levels of infection in the lamina propria and epithelium in hosts infected with wild-type or N4-blind MV. Infection levels were measured in 135 views of tracheas of MV-infected hosts and 169 views of tracheas of N4-blind MV-infected hosts. See Table 1 for the detailed results for each host.

DISCUSSION

MV is the human virus with the highest reproductive rate in naïve populations (20). Its contagion proficiency was recently accounted for by host exit through a receptor expressed in the tracheobronchial epithelium, a strategic location for aerosol droplet release through coughing and sneezing (15, 19). However, how MV reaches this and other epithelia was not understood. To characterize the mechanisms of viral spread within a primate, we infected cynomolgus monkeys with either a wild-type MV or a derivative of this virus that is unable to enter nectin-4-expressing cells because of the targeted mutation of two hemagglutinin residues. As observed previously in rhesus monkeys (21), competence to infect epithelial cells barely affected the initial phases of infection but correlated with more rapid virus clearance and impaired shedding into the upper respiratory tract. These observations confirm the model of infection suggesting that MV attacks the im-

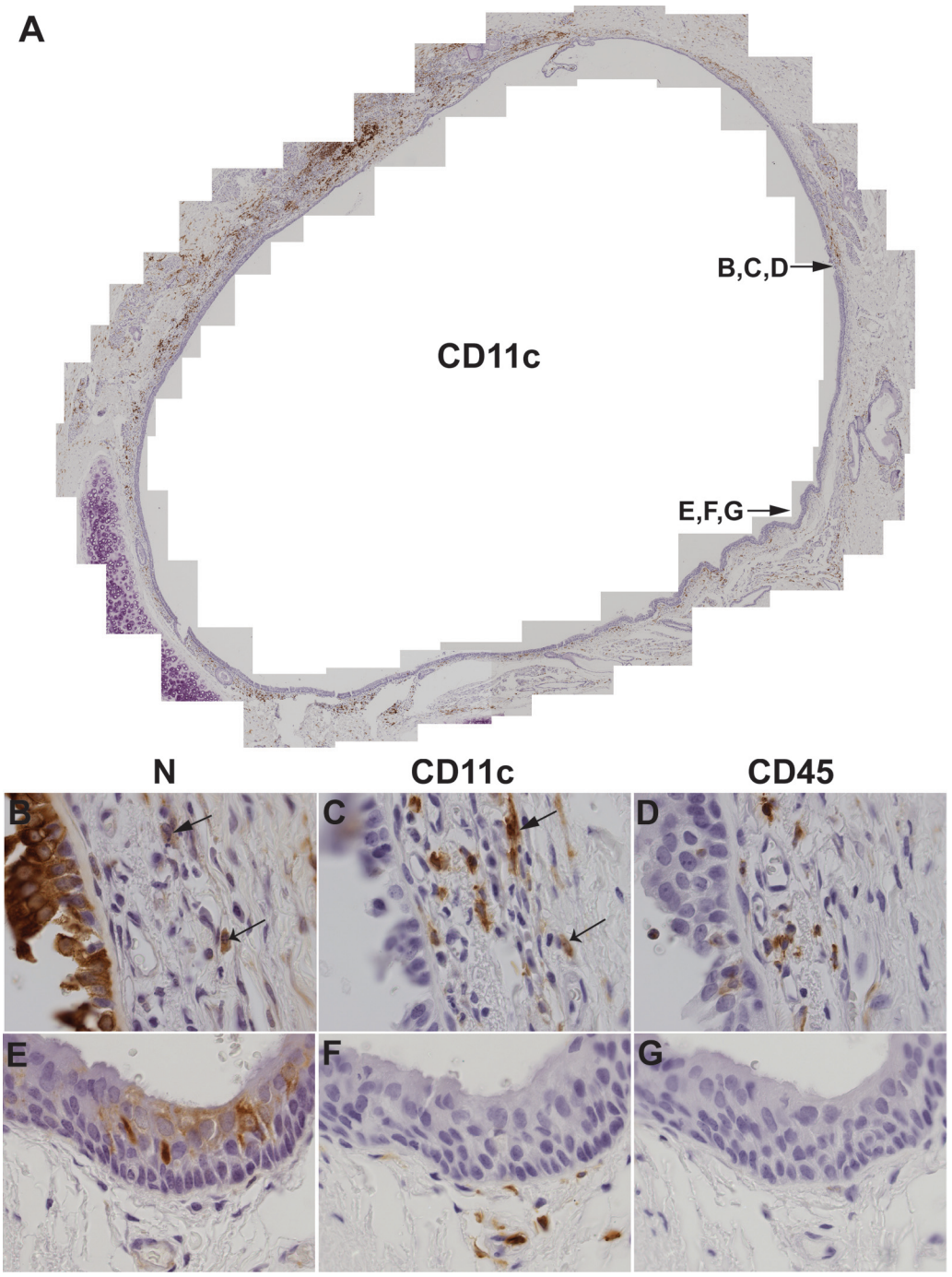

FIG 7 Distributions of $CD11c^+$, $CD45^+$, and $nucleocapsid^+$ cells in the trachea. Consecutive paraffin-embedded tracheal sections from wild-type MV-infected animals were stained with monoclonal antibodies recognizing CD11c (A, C, and F), MV N (B and E), or CD45 (D and G) and counterstained with hematoxylin. The slide order was CD11c, nucleocapsid, and CD45. Antibody reactions were visualized with the brown chromogen DAB. Composite pictures were assembled from overlapping areas photographed at a magnification of ×200 or ×1,000. The locations of the areas in the panel are indicated in the composite overview.

mune system first and then spreads to the epithelium of the airways (21, 25). They also highlight a role of epithelial cell infection in maintaining immune cell infection at later disease stages, on one hand by serving as a reservoir for the infection of newly generated immune cells and on the other by aggravating infection control due to the increased number of infected cells to be eliminated.

This infection model was recently validated for another member of the *Morbillivirus* genus, canine distemper virus (CDV). To generate a virus incapable of epithelial spread (26, 27), the MV hemagglutinin mutations impairing nectin-4-dependent cell entry were transferred to the hemagglutinin of a CDV causing lethal disease in ferrets (27). Animal studies confirmed the importance of epithelial cell infection for virus shedding and revealed that

incompetence to infect epithelia prevented development of rash, fever, and gastrointestinal clinical signs (27). Thus, for CDV virulence in ferrets, nectin-4-dependent spread has more severe consequences than it does for MV virulence in monkeys. This is consistent with more widespread nectin-4 expression in dog cells (28).

The use of airway macrophages and dendritic cells as vehicles to cross the epithelial barrier during early MV infection stages is well documented (10, 29). Moreover, other systemic viruses that are transmitted by aerosol may use myeloid cells to initiate systemic spread (30, 31). Here we observed that immune cells infiltrating the basal lamina of the trachea might serve as vehicles for MV spread to epithelia, which is required for host exit. Close contacts between infected immune cells and epithelial cells create opportunities for cell-cell fusion upon binding of the viral hemagglutinin expressed on the surfaces of infected immune cells to nectin-4 expressed at adherens junctions of epithelial cells. While nectin-4 is expressed at high levels only in the human trachea, its expression is also detected in other tissues, including the lungs and skin (17, 18). Infected immune cells could spread the infection to all of these tissues.

These observations raise new questions regarding the nature of the immune cell populations used as vehicles and how these cells relate to the vehicles used for crossing the epithelial barrier in the opposite direction immediately after contagion. While these questions will be addressed in future studies, we note that synapse-like interfaces have been observed between MV-infected dendritic cells and lymphocytes (32) and that analogous structures may form in epithelia.

Finally, a nectin-4-blind virus may become part of the MV eradication strategy. The exposure of naïve individuals to the vaccine virus through contact with shedding vaccinees is a challenge in the ongoing polio eradication campaign and is a recognized risk of the smallpox vaccine (33, 34). While a safe and efficient inactivated polio vaccine is available, efforts to develop an inactivated MV vaccine ceased in the 1960s, after a formalin-inactivated formulation was associated with more severe disease (35). The lack of shedding associated with the N4-blind MV observed here and the complete absence of clinical disease seen in ferrets infected with a nectin-4-blind CDV (27) provide proof of concept for the use of N4-blind MV during the late stages of the eradication campaign, when accidental transmission to naïve contacts can become increasingly problematic.

ACKNOWLEDGMENTS

We thank Chantal Thibault and Isabelle Meunier for technical support and help with the animal experiments, Marie-Chantal Desrosiers and Louise Gaudet for surgical assistance, Jocelyn Fournier and Gary Kobinger for facilitating the macaque studies, and Tanner Miest for help with compiling data.

This work was supported by grants NIH R01 AI063476 to R.C. and CIHR MOP-66989 and CFI 9488 to V.V.M. X.X.W. was supported by a CIHR Master's Award. M.M. is a Merck Fellow of the Life Sciences Research Foundation.

REFERENCES

1. **Nature.** 2011. Vaccines: the case of measles. Nature **473**:434–435.
2. **Chen SY, Anderson S, Kutty PK, Lugo F, McDonald M, Rota PA, Ortega-Sanchez IR, Komatsu K, Armstrong GL, Sunenshine R, Seward JF.** 2011. Health care-associated measles outbreak in the United States after an importation: challenges and economic impact. J. Infect. Dis. **203**:1517–1525.
3. **Moss WJ, Griffin DE.** 2012. Measles. Lancet **379**:153–164.
4. **Klinkenberg D, Nishiura H.** 2011. The correlation between infectivity and incubation period of measles, estimated from households with two cases. J. Theor. Biol. **284**:52–60.
5. **Bellini WJ, Rota PA.** 2011. Biological feasibility of measles eradication. Virus Res. **162**:72–79.
6. **de Swart RL.** 2009. Measles studies in the macaque model. Curr. Top. Microbiol. Immunol. **330**:55–72.
7. **McChesney MB, Miller CJ, Rota PA, Zhu YD, Antipa L, Lerche NW, Ahmed R, Bellini WJ.** 1997. Experimental measles. I. Pathogenesis in the normal and the immunized host. Virology **233**:74–84.
8. **de Swart RL, Ludlow M, de Witte L, Yanagi Y, van Amerongen G, McQuaid S, Yuksel S, Geijtenbeek TB, Duprex WP, Osterhaus AD.** 2007. Predominant infection of CD150+ lymphocytes and dendritic cells during measles virus infection of macaques. PLoS Pathog. **3**:e178. doi:10.1371/journal.ppat.0030178.
9. **Devaux P, Hodge G, McChesney MB, Cattaneo R.** 2008. Attenuation of V- or C-defective measles viruses: infection control by the inflammatory and interferon responses of rhesus monkeys. J. Virol. **82**:5359–5367.
10. **Lemon K, de Vries RD, Mesman AW, McQuaid S, van Amerongen G, Yuksel S, Ludlow M, Rennick LJ, Kuiken T, Rima BK, Geijtenbeek TB, Osterhaus AD, Duprex WP, de Swart RL.** 2011. Early target cells of measles virus after aerosol infection of non-human primates. PLoS Pathog. **7**:e1001263. doi:10.1371/journal.ppat.1001263.
11. **Leonard VH, Hodge G, Reyes-Del Valle J, McChesney MB, Cattaneo R.** 2010. Measles virus selectively blind to signaling lymphocytic activation molecule (SLAM; CD150) is attenuated and induces strong adaptive immune responses in rhesus monkeys. J. Virol. **84**:3413–3420.
12. **Tatsuo H, Ono N, Tanaka K, Yanagi Y.** 2000. SLAM (CDw150) is a cellular receptor for measles virus. Nature **406**:893–897.
13. **de Vries RD, Lemon K, Ludlow M, McQuaid S, Yuksel S, van Amerongen G, Rennick LJ, Rima BK, Osterhaus AD, de Swart RL, Duprex WP.** 2010. In vivo tropism of attenuated and pathogenic measles virus expressing green fluorescent protein in macaques. J. Virol. **84**:4714–4724.
14. **de Vries RD, McQuaid S, van Amerongen G, Yuksel S, Verburgh RJ, Osterhaus AD, Duprex WP, de Swart RL.** 2012. Measles immune suppression: lessons from the macaque model. PLoS Pathog. **8**:e1002885. doi:10.1371/journal.ppat.1002885.
15. **Muhlebach MD, Mateo M, Sinn PL, Prufer S, Uhlig KM, Leonard VH, Navaratnarajah CK, Frenzke M, Wong XX, Sawatsky B, Ramachandran S, McCray PBJ, Cichutek K, von Messling V, Lopez M, Cattaneo R.** 2011. Adherens junction protein nectin-4 is the epithelial receptor for measles virus. Nature **480**:530–533.
16. **Noyce RS, Bondre DG, Ha MN, Lin LT, Sisson G, Tsao MS, Richardson CD.** 2011. Tumor cell marker PVRL4 (nectin 4) is an epithelial cell receptor for measles virus. PLoS Pathog. **7**:e1002240. doi:10.1371/journal.ppat.1002240.
17. **Reymond N, Fabre S, Lecocq E, Adelaide J, Dubreuil P, Lopez M.** 2001. Nectin4/PRR4, a new afadin-associated member of the nectin family that trans-interacts with nectin1/PRR1 through V domain interaction. J. Biol. Chem. **276**:43205–43215.
18. **Brancati F, Fortugno P, Bottillo I, Lopez M, Josselin E, Boudghene-Stambouli O, Agolini E, Bernardini L, Bellacchio E, Iannicelli M, Rossi A, Dib-Lachachi A, Stuppia L, Palka G, Mundlos S, Stricker S, Kornak U, Zambruno G, Dallapiccola B.** 2010. Mutations in PVRL4, encoding cell adhesion molecule nectin-4, cause ectodermal dysplasia-syndactyly syndrome. Am. J. Hum. Genet. **87**:265–273.
19. **Racaniello V.** 2011. Virology: an exit strategy for measles virus. Science **334**:1650–1651.
20. **Monto AS.** 1999. Interrupting the transmission of respiratory tract infections: theory and practice. Clin. Infect. Dis. **28**:200–204.
21. **Leonard VH, Sinn PL, Hodge G, Miest T, Devaux P, Oezguen N, Braun W, McCray PBJ, McChesney MB, Cattaneo R.** 2008. Measles virus blind to its epithelial cell receptor remains virulent in rhesus monkeys but cannot cross the airway epithelium and is not shed. J. Clin. Invest. **118**:2448–2458.
22. **Ono N, Tatsuo H, Hidaka Y, Aoki T, Minagawa H, Yanagi Y.** 2001. Measles viruses on throat swabs from measles patients use signaling lymphocytic activation molecule (CDw150) but not CD46 as a cellular receptor. J. Virol. **75**:4399–4401.
23. **Hashimoto K, Ono N, Tatsuo H, Minagawa H, Takeda M, Takeuchi K, Yanagi Y.** 2002. SLAM (CD150)-independent measles virus entry as re-

vealed by recombinant virus expressing green fluorescent protein. J. Virol. **76**:6743–6749.
24. **Takeda M, Takeuchi K, Miyajima N, Kobune F, Ami Y, Nagata N, Suzaki Y, Nagai Y, Tashiro M.** 2000. Recovery of pathogenic measles virus from cloned cDNA. J. Virol. **74**:6643–6647.
25. **Takeda M.** 2008. Measles virus breaks through epithelial cell barriers to achieve transmission. J. Clin. Invest. **118**:2386–2389.
26. **Langedijk JP, Janda J, Origgi FC, Orvell C, Vandevelde M, Zurbriggen A, Plattet P.** 2011. Canine distemper virus infects canine keratinocytes and immune cells by using overlapping and distinct regions located on one side of the attachment protein. J. Virol. **85**:11242–11254.
27. **Sawatsky B, Wong XX, Hinkelmann S, Cattaneo R, von Messling V.** 2012. Canine distemper virus epithelial cell infection is required for clinical disease but not for immunosuppression. J. Virol. **86**:3658–3666.
28. **Pratakpiriya W, Seki F, Otsuki N, Sakai K, Fukuhara H, Katamoto H, Hirai T, Maenaka K, Techangamsuwan S, Lan NT, Takeda M, Yamaguchi R.** 2012. Nectin4 is an epithelial cell receptor for canine distemper virus and involved in neurovirulence. J. Virol. **86**:10207–10210.
29. **Ferreira CS, Frenzke M, Leonard VH, Welstead GG, Richardson CD, Cattaneo R.** 2010. Measles virus infection of alveolar macrophages and dendritic cells precedes spread to lymphatic organs in transgenic mice expressing human signaling lymphocytic activation molecule (SLAM, CD150). J. Virol. **84**:3033–3042.
30. **Zaucha GM, Jahrling PB, Geisbert TW, Swearengen JR, Hensley L.** 2001. The pathology of experimental aerosolized monkeypox virus infection in cynomolgus monkeys (Macaca fascicularis). Lab. Invest. **81**:1581–1600.
31. **Papaioannou N, Billinis C, Psychas V, Papadopoulos O, Vlemmas I.** 2003. Pathogenesis of encephalomyocarditis virus (EMCV) infection in piglets during the viraemia phase: a histopathological, immunohistochemical and virological study. J. Comp. Pathol. **129**:161–168.
32. **Koethe S, Avota E, Schneider-Schaulies S.** 2012. Measles virus transmission from dendritic cells to T cells: formation of synapse-like interfaces concentrating viral and cellular components. J. Virol. **86**:9773–9781.
33. **Wagner BG, Earn DJ.** 2008. Circulating vaccine derived polio viruses and their impact on global polio eradication. Bull. Math. Biol. **70**:253–280.
34. **Wertheimer ER, Olive DS, Brundage JF, Clark LL.** 2012. Contact transmission of vaccinia virus from smallpox vaccinees in the United States, 2003–2011. Vaccine **30**:985–988.
35. **Fulginiti VA, Eller JJ, Downie AW, Kempe CH.** 1967. Altered reactivity to measles virus. Atypical measles in children previously immunized with inactivated measles virus vaccines. JAMA **202**:1075–1080.